

# A novel optimizing PI control of shunt active power filter for power quality enhancement

Ayad Mahmood Hadi, Ekhlas M. Thajeel, Ali K. Nahar

Department of Electrical Engineering, University of Technology–Iraq, Baghdad, Iraq

## Article Info

### Article history:

Received Oct 4, 2021

Revised Mar 25, 2022

Accepted Apr 18, 2022

### Keywords:

Lévy flight distribution  
algorithm

p-q theory

PWM

SAPF

THD

## ABSTRACT

In this paper, shunt active power filter (SAPF) is designed to address the problem of current harmonics in the source current arising from a nonlinear load and improve the quality of electric power. That will be by compensating reactive power and harmonic currents. The PI controller responsible for DC-link energy storage tuning was developed using the Lévy flight distribution algorithm (LFA). It is a novel, previously unused optimization approach to suggest relative gain  $K_p$  and integration gain  $K_i$  gain values for the PI controller. This approach aims to get the best dynamic performance of SAPF, speed up the convergence rate, get the fastest best stability and bypass constant voltage advancement for DC-link. The model was tested and implemented in MATLAB simulation software. The result of total harmonic distortion THD showed the efficiency of this method compared with the results of traditional PI. The design of the model in the current reference frame was based on instantaneous reactive power (pq) theory.

This is an open access article under the [CC BY-SA](#) license.



## Corresponding Author:

Ayad Mahmood Hadi

Department of Electrical Engineering, University of Technology – Iraq

Baghdad, Iraq

Email: eee.19.50@grad.uotechnology.edu.iq

## 1. INTRODUCTION

The increasing use of non-linear loads represented by electronic transformers and various electronic devices led to major problems in the power system, corresponding to the increase in harmonics. It negatively affects the quality of electrical energy, a decrease in the power factor, and poor efficiency of electric power [1]. Harmonics of the higher order of the power lead to additional losses such as heat problems, turbulence, and equipment failure [2]. A reason for the formation of harmonics in non-linear loads is represented in electronic power transformers. As a result of the properties of these electronics in crystal vibration and the effect of the fast-switching process which arises from this fast-switching angle ( $\alpha$ ). As a result of the dynamic and electromagnetic fast response in each oscillation through the wave during the operation process, due to the greatest and increasing need for power electronics devices [3], it is flexible in operation and less maintenance. Therefore, it is necessary to take procedures, methods, and a mechanism for dealing with the harmonics resulting from these devices. The passive power filters can be used to remove harmonics of the electric current wave of the source resulting from these devices and solve their problems; this method has many negatives and problems such as resonance, electromagnetic echo, increased reactive power, and others, to avoid the problems associated with the use of passive filters, the use of active power filters (APF) were used, which represents the best solution for treating harmonics in the electric current, and it is better than traditional passive filters in this performance [4]. The shunt active power filter (SAPF) helps in correcting the current waveform, reducing harmonics, obtaining a wave as close as possible to the sinusoidal shape, compensating the reactive power, and eliminating unwanted frequencies, and therefore; its use has increased widely [5]. The SAPF device is connected in parallel with the network between the source and the load at the common coupling point (PCC),

as shown in Figure 1 and works on the principle of harmonic sensing in the source current wave and generates a compensated current injected into the network to get the best results we use different control strategies as indicated by the literary references and their development Including methods for calculating power, current, and pulse gate generation techniques for pulse width modulation (PWM) of the DC-AC inverter, to achieve the proper compensated harmonic current (SAPF) injection into the network, it is necessary to track the source current and filter current and maintain the voltage via DC-link taking into account the use of time-domain as well as frequency domain. The compensated current is generated by analyzing the distorted voltage and the source current signal and separating the harmonics using real-time analytics [6]. A time-domain approach is used for ease of use in the design of the controller compared to the frequency domain. The current reference frame is based on instantaneous reactive power (pq) theory, which is one of the control methods in the time domain approach, where the voltage difference and harmonic current are calculated to estimate the compensated reference current. Used for power and current calculations. It is one of the commonly used methods. The strategy of controlling source voltage (DC) of the inverter and comparison with constant voltage is using PI, this model was developed by optimizing the performance of the PI controller, which is responsible for tuning the energy storage in DC-link, using the Lévy flight distribution algorithm (LFA), a new optimization method for suggesting Kp and Ki gain values is suitable for the controller to improve the dynamic performance of the SAPF and maintain the required voltage level via DC-link and to obtain the best possible result for total harmonic distortion THD compared to the traditional PI control system and various improvement methods for other researchers. The model was tested and the results verified in MATLAB simulation software. The system under study is a three-phase three-wire system consisting of a three-phase voltage source for the alternating current and non-linear load that represented by electronic devices or electronic power inverters, shunt active power filter (SAPF), and network impedance as shown in Figure 1 [7], [8]. Active power filter consists of a PWM inverter type VSI voltage source inverter fed from a DC source. The APF is connected in parallel between an alternating voltage source and a load at the common coupling point (PCC) in which the equation of the following currents is fulfilled:

$$I_f = I_L - I_s \quad (1)$$

where  $I_f$  represent filter's current,  $I_L$  is load's current and  $I_s$  is source's current.

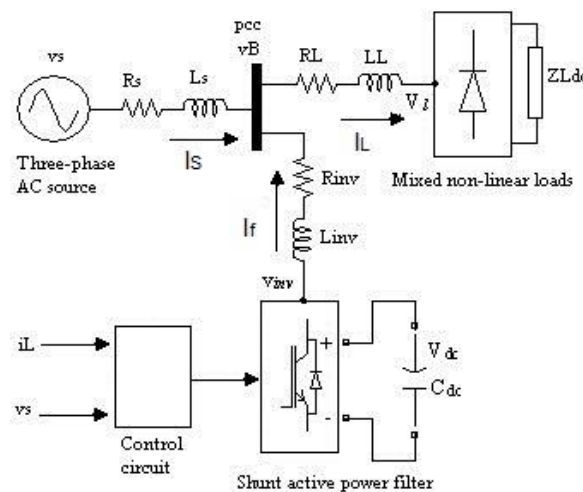


Figure 1. Block diagram of the SAPF

## 2. CURRENT REFERENCE GENERATION TECHNIQUES

In this study, the active power filter (SAPF) was designed by adopting the pq reactive power theory (Akagi, Kanazawa, and Nabae in 1983-1984) in power calculations and generating reference currents [9], [10]. This method is valid for the operation of the SAPF device in the transitional or steady-state and general voltage state because it depends on the time-domain approach and simultaneous detection method as shown in Figure 2. Allow the SAPF device to control in real-time because of the simplicity of the calculations [11]. This method includes only algebraic equations. The compensated harmonic current is generated by analyzing the buffer voltage and current distorting harmonics and separating the harmonics using instantaneous transforms [12].

The calculations of the pq method include only algebraic equations for the counting of the compensated reference current arising in a SAPF device built in a three-phase system. Below, shows the equations of Clark transformations for voltage source and load current in coordinates a b c to binary coordinates

in the following relations [13]. Clark's calculations method uses the two-stage calculation method to convert the three-phase a, b, c measurements to the  $\alpha$  and  $\beta$  two-phase model according to (2) and (3). And reverse this conversion, as shown in (2) and (3) [14].

$$\begin{bmatrix} V\alpha \\ V\beta \end{bmatrix} = \sqrt{\frac{2}{3}} \begin{bmatrix} 1 & -0.5 & -0.5 \\ 0 & \frac{\sqrt{3}}{2} & -\frac{\sqrt{3}}{2} \end{bmatrix} \begin{bmatrix} Va \\ Vb \\ Vc \end{bmatrix} \quad (2)$$

$$\begin{bmatrix} I\alpha \\ I\beta \end{bmatrix} = \sqrt{\frac{2}{3}} \begin{bmatrix} 1 & -0.5 & -0.5 \\ 0 & \frac{\sqrt{3}}{2} & -\frac{\sqrt{3}}{2} \end{bmatrix} \begin{bmatrix} Ia \\ Ib \\ Ic \end{bmatrix} \quad (3)$$

The real power  $P$  and the apparent power  $Q$  are calculated as shown in (4), (5)

$$\begin{bmatrix} P \\ Q \end{bmatrix} = \begin{bmatrix} V\alpha & V\beta \\ V\beta & -V\alpha \end{bmatrix} \begin{bmatrix} I\alpha \\ I\beta \end{bmatrix} \quad (4)$$

where

$$\Delta P = \bar{P} + \tilde{P} \quad (5)$$

where  $\Delta P$  is represents the average components of real power,  $\tilde{P}$  is AC component of  $P$ ,  $\bar{P}$  is DC component.

$$\begin{bmatrix} I\alpha^* \\ I\beta^* \end{bmatrix} = \frac{1}{V\alpha^2 + V\beta^2} \begin{bmatrix} V\alpha & V\beta \\ V\beta & -V\alpha \end{bmatrix} \begin{bmatrix} \Delta P \\ Q \end{bmatrix} \quad (6)$$

$$\begin{bmatrix} I\alpha^* \\ I\beta^* \\ I\gamma^* \end{bmatrix} = \sqrt{\frac{2}{3}} \begin{bmatrix} 1 & 0 \\ -0.5 & \frac{\sqrt{3}}{3} \\ -0.5 & -\frac{\sqrt{3}}{3} \end{bmatrix} \begin{bmatrix} I\alpha^* \\ I\beta^* \end{bmatrix} \quad (7)$$

The output current in (7) represents the three-phase compensating current and it is an obligatory model of the three-phase PWM inverter, the above equation represents the application of the inverse Clark's transforms [15].

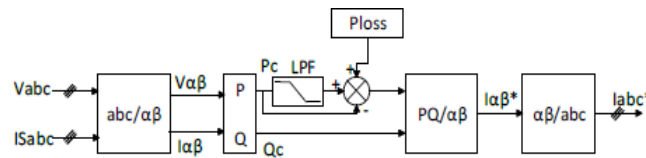


Figure 2. Block diagram of the instantaneous reactive power theory [5]

### 3. HYSTERESIS BAND CURRENT CONTROLLER HBCC

The hysteresis band current control technique is employed to control the compensated currents and select the switching signals for suitable VSI inverter gates. It is also because of the high accuracy, simple operation and independence of parameter variation [16]. The calculations of this model depend on the value of the error function in the current, which represents the difference between the source current and the compensated current injected into the network in (8) [17].

$$e(t) = I_{ref}(t) - I_{inj}(t) \quad (8)$$

Figure 3 shows the working principle of this model on the comparison between the error function and the hysteresis band, as the difference between the reference current and the compensated current is more than the hysteresis band. The lower switching is turned on and the upper switching of the inverter is turned off, as a result, the current begins to fade away [18]. When the difference between the reference current and the compensated current is greater than the lower limit of the hysteresis band, the upper switching is turned on and the lower switching of the compensator is turned off, as a result, the current returns to the hysteresis band. The function (9) shows the conversion performance [19].

$$s = \begin{cases} 0 & \text{if } I_{inj} > I_{ref} + HB \\ 1 & \text{if } I_{inj} < I_{ref} - HB \end{cases} \quad (9)$$

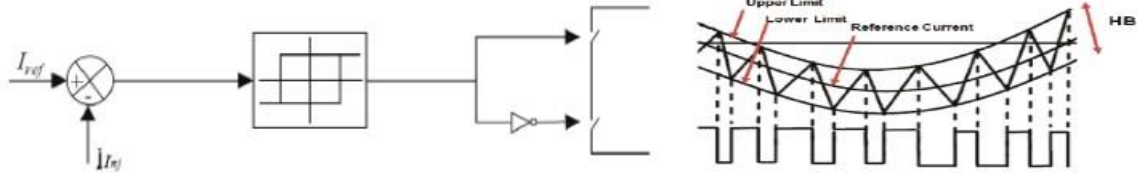


Figure 3. Hysteresis comparatar

#### 4. DC LINK VOLTAGE CONTROL

The PI-type controller is used in the SAPF active power filter to regulate the DC-link voltage and the Lévy flight distribution algorithm is used to optimize the energy storage of the DC voltage in the capacitor based on the processing of the change in DC voltage  $E(t)$  to adjust the parameters of the controller  $K_p$  and  $K_i$  of in order control to progress the dynamic performance and obtain a stable state of the system, as shown in the Figure 4 [20].

$$C(s) = Kp + \frac{Ki}{s} \quad (10)$$

where  $K_p$  represents the relative gain and provides the best dynamic performance, and  $K_i$  represents the integration gain that erases the error in the steady state. Use the traditional method the coefficients of the  $K_p$  and  $K_i$  controllers are calculated by comparing the system's total transfer function with the second-order generalized transfer [21].

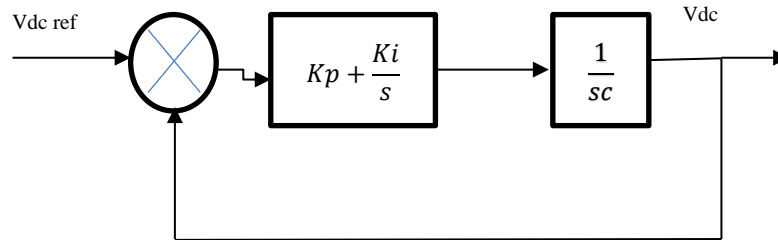


Figure 4. Voltage control loop

In the private accounts of the shunt system active power filter pi control is necessary to set the  $P_{losses}$  used in pq accounts as shown in (11) [22].

$$\bar{P}_{losses} = Kp\Delta V_{dc} + Ki \int \Delta V_{dc} dt \quad (11)$$

where  $P_{loss}$  represents the average loss that occurs inside the VSI transformer carried from the DC-bus link and is intended to give a good response and a suitable compensation where the real DC bus voltage ( $V_{dc}$ ) is compared to the reference ( $V_{dc}^*$ ) and it is managed by the PI controller [23]. In this article, the target function is the error resulting from comparing the source  $V_{dc}$  and the voltage via DC-link. The control PI represents the flight position of the Lévy flight. The goal is to find the values of the constants  $K_p$ ,  $K_i$ , and the error rate must be reduced [24].

In the mathematical model of the simulation environment [25], it is represented as a network environment of wireless sensors in its area. The algorithm's computational mechanisms start from calculating the Euclidean distance ED between each two adjacent sensor points and then determines if the sensor node is by the algorithm based on the calculated distance ED or moving it in another position. A new LFS model will be used elsewhere for a lower sensor node near the search spaces to reduce the occurrence of interference between the sensor nodes. Mathematically, the Lévy flight algorithm calculates the Euclidean distance ED between two adjacent sites, one being  $X_i$  and the other  $X_j$  using (12)

$$ED(X_i; X_j) = \sqrt{(x_i - x_j)^2 + (y_i - y_j)^2} \quad (12)$$

where  $(x_i, y_i)$  is the position coordinate of  $X_i$  and  $(x_j, y_j)$  is the  $X_j$  position coordinate. If the resultant distance is less than the threshold (this means there is a problem in deploying the agents in the search space), then the algorithm starts its mechanism by adjusting the positions of these agents using (13),

$$X_j(t+1) = Levy\_Flight(X_j(t); X_{leader}LB; UB) \quad (13)$$

The  $t$  is an index for the number of iterations.  $Levy\_Flight$  is a function that performs the work of Lévy flights in terms of the step length and direction.  $X_j(t+1)$  illustrates the pseudo-code of this function.  $UB$  and  $LB$  are the highest and lowest values in the 2D dimensions of the search space. Respectively, the  $X_{Leader}$  is the position of agent that has the lowest number of neighbors and will be used as the LF direction. Equation (14) moves the agent  $X_j$  towards the agent's position that has the lowest number of neighbors.

$$X_j(t+1) = LB + (UB - LB)rand(n) \quad (14)$$

$rand(n)$  is a function used to produce random numbers  $R$  in uniform distribution  $[0, 1]$ . In (15), offer more opportunities to discover solutions for unvisited sites in the search space and increases the exploration stage of the proposed algorithm. This equation updates the position of  $X_j$  to a new region in the search space where there are no other agents.

$$R = rand(n).CSV = 0.5 \quad (15)$$

In each update for the  $X_j$  position, CSV is the comparison scalar value with  $R$ . The method examines the value of  $R$  in (15). At each iteration to update the sensor node  $X_j$  location (16). If the value is smaller than CSV in (14). If this is not the case, use (15) to give the algorithm additional chances to find the search space. The potential to explore and improve the algorithm's performance will be enhanced by varying the algorithm's solutions. The suggested approach uses to update  $X_i$  location. In (16) calculates  $X_i$ 's new position, whereas (17) calculates  $X_i$ 's ultimate position.

$$X_i(t+1) = TP + \alpha_1 \times TF_{Neighbours} + rand(n) \times \alpha_2 \times ((TP + \alpha_3 X_{Leader})/2 - X_i(t)) \quad (16)$$

$$X_{New_i}(t+1) = Levy_{Flight}(X_i(t+1).TP.LB.UB) \quad (17)$$

$TP$  is the position (solution) that obtained the greatest fitness value of the objective function, which is termed the target position, and Lévy flight is a function illustrated in (13). The random numbers 1, 2, and 3 are arranged in such a way that 0, 1, 2, 3 equals 10.  $TF$  neighbours surrounding  $X_i(t)$  have a total goal fitness of  $TF$  neighbours.

$$TF\_NEIGHBOURS = \sum_{K=1}^{NN} \frac{D(k) \times X_k}{NN} \quad (18)$$

where  $X_k$  denotes  $X_i$  national's position,  $K$  denotes the neighbor's index,  $NN$  is the total number of  $X_i$  national's and  $D(K)$  denotes the fitness score for each vicinity.

$$D(k) = \frac{\partial_1(V - \min(V))}{\max(V) - \min(V)} + \partial_2 \quad (19)$$

where,

$$V = \frac{Fitness(X_j(t))}{Fitness(X_i(t))}, \text{ and } 0 < \partial_1, \partial_2 \leq 1 \quad (20)$$

The suggested LFD method is depicted with the above equation. Each iteration of the LFD algorithm will repeat all of the previously stated equations. Assume that  $t$  represents the total number of iterations and  $n$  represents number of agents

## 5. SIMULATION AND RESULT

The simulation results for the designed model show an excellent compensation for the source harmonic current and an ideal compensation for SAPF. The model suggested had been implemented in a MATLAB simulation model, and a validation of the effectiveness of the designed PI controller in maintaining DC voltage across both ends of the capacitor with balanced load conditions. The specification parameters used in designing the model are listed in Table 1. The objective function is reduced by optimizing the PI parameters, the DC-link voltage control model is designed and the objective function is minimized by using optimization techniques, in this model, the Lévy flight determination algorithm was used, it is vital to set the search space to improve the parameters of the PI console, which are  $K_p$ ,  $K_i$ , and get the best results. The search space can be specified for parameter  $0.1 \leq K_p \leq 20$ , the search space for parameter  $K_i$   $10 \leq K_i \leq 200$ , the number of agents

10, and the number of iterations 10, we have run different simulations with the number of iterations to get an optimal value of the parameters of. Source stream analysis by fast Fourier series obtained from simulation in MATLAB. Simulation results for THD are included in Table 2 for the different cases before and after using the filter and when using the optimization method. The source current wave before filtering is shown in Figure 5, and the load current before the filtering process in Figure 6 shows the extent of harmonic distortion. The THD of the source current before using the filter is 24.44% as shown in Figure 7 spectrum analysis of the source current. When using SAPF; While the compensator currents shown in Figure 8 that are pumped. The change in the wave form of the source current is obvious after filtering compared to the wave form of the load and filter current as shown in Figure 9. When using a conventional PI system, the THD decreases to 4.62% as shown in Figure 10. Also optimizing the operation of the PI control system, using a Lévy flight distribution algorithm graph, the THD of the source current is reduced to 1.56% as shown in Figure 11, and its waveform is as close as possible to the pure sine wave compared to its distortion.

Table 1. Specifications of model design parameter

| Specifications                         | Parameters   | Values       |
|--|--------------|--------------|
| Supply phase voltage (RMS)             | $V_s$        | 220 V, 50 Hz |
| Line inductor                          | $L_{ac}$     | 3 mH         |
| Nonlinear load                         | Diode bridge | 63 A         |
| DC-link voltage                        | $V_{dc}$     | 620 voltage  |
| DC inductor                            | $L_{dc}$     | 1.6 mH       |
| DC capacitor                           | $C_{dc-equ}$ | 1.0 mF       |
| DC load: constant power resistive load | $R_L$        | 40 $\Omega$  |

Table 2. Simulation results of model

| Control technique | Before using SAPF | After using SAPF (Conventional PI) | Using PI controller with (LFA) |
|-------------------|-------------------|------------------------------------|--------------------------------|
| THD               | 24.44%            | 4.62%                              | 1.56%                          |

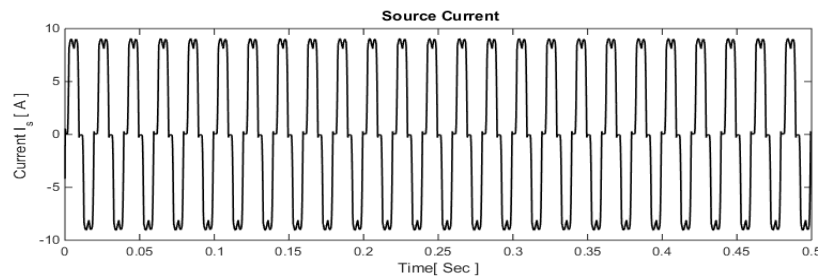


Figure 5. Source current without filter

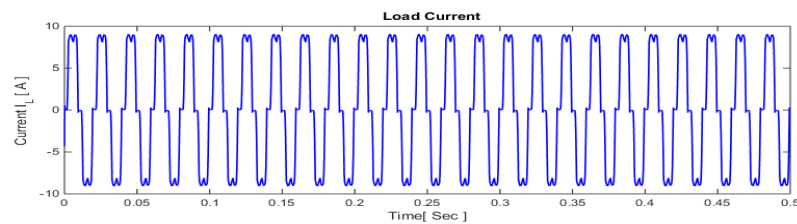


Figure 6. Load current

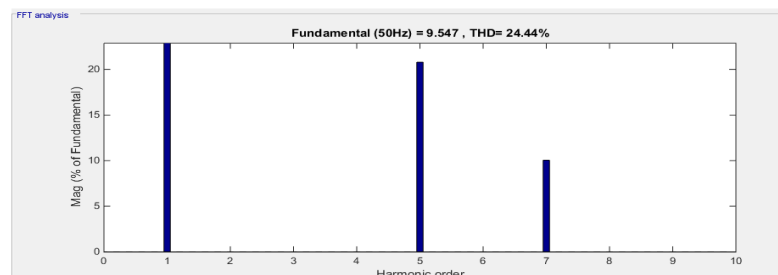


Figure 7. Source current spectrum without filter

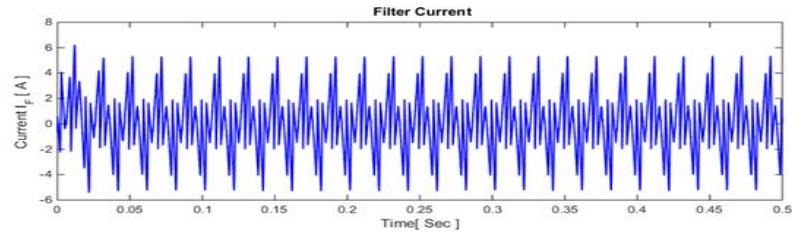


Figure 8. Filter current

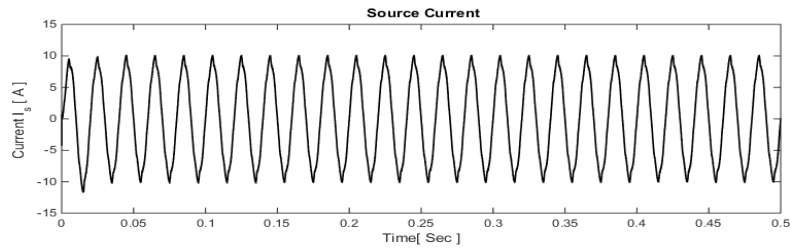


Figure 9. Source current after using SAPF

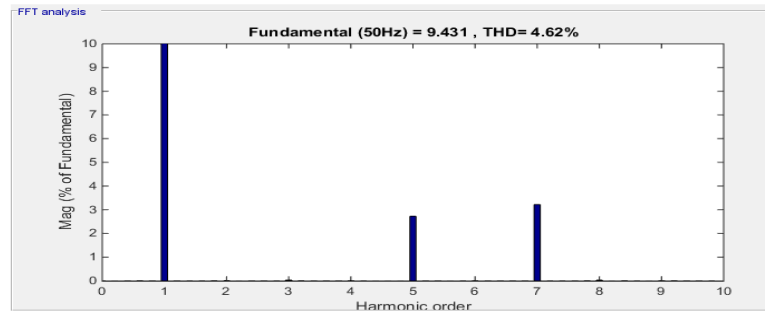


Figure 10. Source current spectrum with filter (PI conventional)

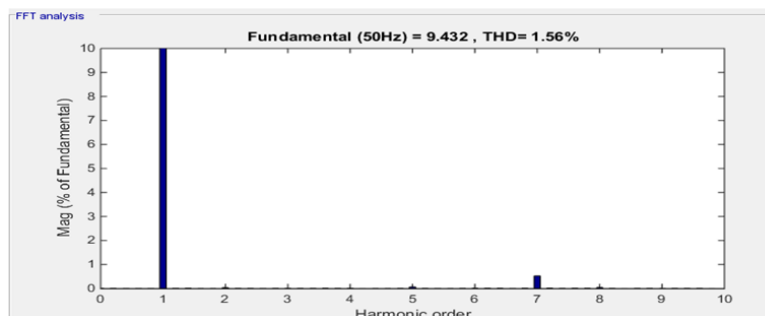


Figure 11. Source current spectrum with filter (Lévy flights algorithm)

## 6. CONCLUSION

In this research, a group of techniques were used that showed their effects use and obtaining the best results in controlling the SAPF device. The pq theory was used in the current reference generation techniques for the speculative current calculations. The hysteresis band current controller HBCC theory was used to control the transformer device (VSI) within the PWM model. The Lévy flights distribution algorithm is proposed to improve the performance of the DC-link PI control, based on the techniques used in this model to determine the compensated reference current. The proposed model shows excellent performance in the SAPF device. These obtained results showed an increase in the power factor to 98.5 and that the voltage difference across the two ends of the DC. The capacitor is almost constant with a small ripple and that the quality of the source current is in an almost pure sinusoidal waveform after filtering, that the voltage waveform is in the same



phase, and that the voltage waveform is in the same phase, the THD was reduced in the current model from 24.44% to 4.62% in the case of using the filter when improving the performance using the Lévy flight distribution algorithm, the THD was reduced to 1.56%, as the use of this method can be considered as one of the modern and important contributions that are used for the first time in this field and did not address it one of the researchers previously because the innovation of this algorithm is recent.




## REFERENCES

- [1] I. Ali, V. Sharma, and P. Chhawchharia, "CONTROL TECHNIQUES FOR ACTIVE POWER FILTER FOR HARMONIC ELIMINATION & POWER QUALITY IMPROVEMENT," *Int. J. Electr. Electron. Data Commun.*, vol. 4, no. 10, pp. 25–36, 2016.
- [2] M. Kashif *et al.*, "A Fast Time-Domain Current Harmonic Extraction Algorithm for Power Quality Improvement Using Three-Phase Active Power Filter," *IEEE Access*, vol. 8, pp. 103539–103549, 2020, doi: 10.1109/ACCESS.2020.2999088.
- [3] S. Al-Gahtani and R. M. Nelms, "A New Voltage Sensorless Control Method for a Shunt Active Power Filter for Unbalanced Conditions," *Proc. - 2019 IEEE Int. Conf. Environ. Electr. Eng. 2019 IEEE Ind. Commer. Power Syst. Eur. IEEEIC/ CPS Eur. 2019*, no. 2, pp. 1-6, 2019, doi: 10.1109/IEEEIC.2019.8783570.
- [4] B. Rouabah, H. Toubakh, and M. Sayed-Mouchaweh, "Fault tolerant control of multicellular converter used in shunt active power filter," *Electr. Power Syst. Res.*, vol. 188, pp. 1–21, 2020, doi: 10.1016/j.epsr.2020.106533.
- [5] S. H. Mohamad *et al.*, "Adaptive notch filter under indirect and direct current controls for active power filter," *Bulletin of Electrical Engineering and Informatics (BEEI)*, vol. 9, no. 5, pp. 1794–1802, 2020, doi: 10.11591/eei.v9i5.2165.
- [6] Y. Bekakra, L. Zellouma, and O. Malik, "Improved predictive direct power control of shunt active power filter using GWO and ALO – Simulation and experimental study," *Ain Shams Engineering Journal*, vol. 12, no. 4, pp. 3859–3877, 2021, doi: 10.1016/j.asej.2021.04.028.
- [7] A. Amirullah, A. Adiananda, O. Penangsang, and A. Soeprijanto, "Load Active Power Transfer Enhancement Using UPQC-PV-BES System With Fuzzy Logic Controller," *International Journal of Intelligent Engineering and Systems*, vol. 13, no. 2, pp. 329–349, 2020, doi: 10.22266/ijies2020.0430.32
- [8] P. Suresh and G. Vijayakumar, "Shunt Active Power Filter with Solar Photovoltaic System for Long-Term Harmonic Mitigation," *J. Circuits, Syst. Comput.*, vol. 29, no. 5, pp. 1–23, 2020, doi: 10.1142/S0218126620500814
- [9] M. Sellali, S. Abdeddaim, A. Betka, A. Djerdir, S. Drid, and M. Tiar, "Fuzzy-Super twisting control implementation of battery/super capacitor for electric vehicles," *ISA Trans.*, vol. 95, pp. 243–253, 2019, doi: 10.1016/j.isatra.2019.04.029.
- [10] E. Sundaram, M. Gunasekaran, R. Krishnan, S. Padmanaban, S. Chenniappan, and A. H. Ertas, "Genetic algorithm based reference current control extraction based shunt active power filter," *Int. Trans. Electr. Energy Syst.*, vol. 31, no. 1, pp. 1–22, 2021, doi: 10.1002/2050-7038.12623.
- [11] S. Kumaresan and H. H. Sait, "Design and control of shunt active power filter for power quality improvement of utility powered brushless DC motor drives," *Automatika*, vol. 61, no. 3, pp. 507–521, 2020, doi: 10.1080/00051144.2020.1789402.
- [12] A. Srivastava and D. K. Das, "A Whale Optimization Algorithm Based Shunt Active Power Filter for Power Quality Improvement," *Int. J. Electr. Energy*, vol. 6, no. 1, pp. 7–12, 2018, doi: 10.18178/ijoe.6.1.7-12.
- [13] Y. Fang and J. Fei, "Adaptive Backstepping Current Control of Active Power Filter Using Neural Compensator," *Math. Probl. Eng.*, vol. 2019, pp. 1–9, 2019, doi: 10.1155/2019/5130738.
- [14] A. Lakum and V. Mahajan, "A novel approach for optimal placement and sizing of active power filters in radial distribution system with nonlinear distributed generation using adaptive grey wolf optimizer," *Engineering Science and Technology, an International Journal*, vol. 24, no. 4, pp. 911–924, 2021, doi: 10.1016/j.jestch.2021.01.11
- [15] S. Ouchen, M. Benbouzid, F. Blaabjerg, A. Betka, and H. Steinhart, "Direct Power Control of Shunt Active Power Filter using Space Vector Modulation based on Super Twisting Sliding Mode Control," *IEEE J. Emerg. Sel. Top. Power Electron.*, vol. 9, no. 3, pp. 3243–3253, 2020, doi: 10.1109/JESTPE.2020.3007900.
- [16] I. Ullah and M. Ashraf, "Sliding mode control for performance improvement of shunt active power filter," *SN Appl. Sci.*, vol. 1, no. 6, pp. 1–10, 2019, doi: 10.1007/s42452-019-0554-9.
- [17] K. Rameshkumar and V. Indragandhi, "Real Time Implementation and Analysis of Enhanced Artificial Bee Colony Algorithm Optimized PI Control algorithm for Single Phase Shunt Active Power Filter," *Journal of Electrical Engineering & Technology*, vol. 15, no. 4, pp. 1541–1554, 2020, doi: 10.1007/s42835-020-00437-2.
- [18] B. Hu, L. Kang, J. Liu, J. Zhang, S. Wang and Z. Zhang, "Model Predictive Direct Power Control with Fixed Switching Frequency and Computational Amount Reduction," *IEEE J. Emerg. Sel. Top. Power Electron.*, vol. 7, no. 2, pp. 956–966, 2019, doi: 10.1109/JESTPE.2019.2894007.
- [19] D. Buła, D. Grabowski, M. Lewandowski, M. Maciążek, and A. Piwowar, "Software Solution for Modeling, Sizing, and Allocation of Active Power Filters in Distribution Networks," *Energies*, vol. 14, no. 1, pp. 1–25, 2020, doi: 10.3390/en14010133.
- [20] B. P. Narendra, R. B. Peesapati, and G. Panda, "An Adaptive Current Control Technique in Grid-tied PV System with Active Power Filter for Power Quality Improvement," *IEEE Reg. 10 Annu. Int. Conf. Proceedings/TENCON*, pp. 187–191, 2019, doi: 10.1109/TENCON.2019.8929487.
- [21] P. Shukl and B. Singh, "Recursive Digital Filter Based Control for Power Quality Improvement of Grid Tied Solar PV System," *IEEE Trans. Ind. Appl.*, vol. 56, no. 4, pp. 3412–3421, 2020, doi: 10.1109/TIA.2020.2990369.
- [22] M. Klimas, D. Grabowski, and D. Buła, "Application of Decision Trees for Optimal Allocation of Harmonic Filters in Medium-Voltage Networks," *Energies*, vol. 14, no. 4, pp. 1–24, 2021, doi: 10.3390/en14041173.
- [23] R. Belyaevsky and A. Gerasimenko, "Development of Mechanisms for Active-Adaptive Control of Reactive Power Based on Intelligent Electrical Networks," *E3S Web Conf.*, vol. 209, pp. 1–6, 2020, doi: 10.1051/e3sconf/202020902004.
- [24] S. M. Bagi, F. N. Kudchi, and S. Bagewadi, "Power Quality Improvement using a Shunt Active Power Filter for Grid Connected Photovoltaic Generation System," *2020 IEEE Bangalore Humanitarian Technology Conference (B-HTC)*, 2020, doi: 10.1109/B-HTC50970.2020.9298001.
- [25] A. Bielecka and D. Wojciechowski, "Stability Analysis of Shunt Active Power Filter with Predictive Closed-Loop Control of Supply Current," *Energies*, vol. 14, no. 8, pp. 1–17, 2020, doi: 10.3390/en14082208
- [26] E. H. Houssein, M. R. Saad, F. A. Hashim, H. Shaban, and M. Hassaballah, "Lévy flight distribution: A new metaheuristic algorithm for solving engineering optimization problems," *Journal Engineering Applications of Artificial Intelligence*, vol. 94, pp. 1–18, 2020, doi: 10.1016/j.engappai.2020.103731.






## BIOGRAPHIES OF AUTHORS






**Ayad Mahmood Hadi**    Received the B.Sc. degrees in Electrical Engineering from University of Technology, Baghdad, Iraq, in 2006. His research interests include the applications of artificial intelligence techniques to power system planning, operation, and control. He is currently studying a master's degree in electrical power engineering at the University of Technology. He can be contacted at email: eee.19.50@grad.uotechnology.edu.iq.



**Ekhlās M. Thajeel**    was born in Baghdad, Iraq in January of 1973. She received her B.Sc and M.Sc degrees in 1995 and 2005 respectively and PhD (Electrical Engineering) from University Malaysia Pahang (UMP) in 2018. She is currently serves as a Lecturer at Faculty of Electrical & Electronics Engineering, University of Technology (UOT). She has authored and co-authored technical papers in the international journals and conferences and also has been invited as a Journal reviewer for several international journals and conferences in the field of power system, soft computing application. She is also a Member of IEEE. Her website can be accessed through [https://www.researchgate.net/profile/Ekhlās\\_Mhawī](https://www.researchgate.net/profile/Ekhlās_Mhawī). She can be contacted at email: 30091@uotechnology.edu.iq.



**Ali K. Nahar**    was born in Baghdad, Iraq in June of 1979. He received his B.Sc and M.Sc degrees in 2001 and 2008 respectively In University of Baghdad and University of Technology, Iraq. From 2013-2016, he joined a PhD study at the Faculty of Electric Engineering, (UMP), Pahang, Malaysia. Since 2002, he has been a Lecturer of Electronic and communications Engineering at the University of Technology (UOT), Baghdad, Iraq. Starting scientific publishing since 2007, he has more than 25 publications in national and international conferences and journals. He can be contacted at email: 30081@uotechnology.edu.iq.